Conformational Change of Helix G in the Bacteriorhodopsin Photocycle: Investigation with Heavy Atom Labeling and X-Ray Diffraction

Toshihiko Oka,* Hironari Kamikubo,# Fumio Tokunaga,* Janos K. Lanyi,§ Richard Needleman,¶ and Mikio Kataoka*

*Department of Earth and Space Science, and #Department of Physics, Graduate School of Science, Osaka University, Toyonaka 560-0043, Japan; §Department of Biophysics and Physiology, University of California, Irvine, California 92697 USA; and ¶Department of Biochemistry, Wayne State University, Detroit, Michigan 48201 USA

ABSTRACT According to the current structural model of bacteriorhodopsin, Ile^{222} is located at the cytoplasmic end of helix G. We labeled the single cysteine of the site-directed mutant $Ile^{222} \rightarrow Cys$ with *p*-chloromercuribenzoic acid and determined the position of the labeled mercury by x-ray diffraction in the unphotolyzed state, and in the M_N photointermediate accumulated in the presence of guanidine hydrochloride at pH 9.5. According to the difference Fourier maps between the M_N intermediate and the unphotolyzed state, the structural change in the M_N intermediate was not affected by mercury labeling. The difference Fourier map between the labeled and the unlabeled I222C gave the position of the mercury label. This information was obtained for both the unphotolyzed state and the M_N intermediate. We found that the position of the mercury at residue 222 is shifted by 2.1 ± 0.8 Å in the M_N intermediate. This agrees with earlier results that suggested a structural change in the G helix. The movement of the mercury label is so large that it must originate from a cooperative conformational change in the helix G at its cytoplasmic end, rather than from displacement of residue 222. Because Ile^{222} is located at the same level on the *z* coordinate as Asp^{96}, the structural change in the G helix could have the functional role of perturbing the environment and therefore the pK_a of this functionally important aspartate.

INTRODUCTION

Bacteriorhodopsin (BR) is a light-driven proton pump in the purple membrane of *Halobacterium salinarium*. The photocycle of BR is initiated by absorption of a photon by the retinal chromophore. The photocycle can be described as a sequence of states, BR → J → K → L → M → N → O → BR. The important steps for proton transfer in the photocycle are the deprotonation of Schiff base of retinal to D85, located on the extracellular side, which is the L-to-M transition, and the reprotonation of Schiff base from D96, located on the cytoplasmic side, which is the M-to-N transition (reviewed most recently in Lanyi, 1997). Because the deprotonation and the reprotonation are closely related to the release and the uptake of a proton, global conformational change is expected to be part of the switch between the deprotonation and reprotonation steps (Kataoka et al., 1994; Lanyi, 1995, 1997).

The evidence for global structural changes of BR at the M or the N intermediate has come from various laboratories (Dencher et al., 1989; Koch et al., 1991; Nakasako et al., 1991; Subramaniam et al., 1993; Kamikubo et al., 1996; Vonck, 1996). These diffraction studies suggested that major changes occur at helices B, F, and G. Later, it was revealed that the characteristics of the M intermediate are the changes near helices B and G, whereas the characteristics of the N intermediate are the changes near helices F and G (Kamikubo et al., 1997). Fourier transform infrared (FTIR) study of the deprotonated state of D96N at alkaline pH suggested the existence of a substate termed the M_N intermediate, a state that already has the N-type protein conformation, but with a still deprotonated Schiff base (Sasaki et al., 1992). The M_N state was distinguished from the pure M state by x-ray diffraction as well (Kamikubo et al. 1997). A transition between two M substates (M_1 and M_2) has been proposed to account for the extracellular-to-cytoplasmic change in the access of the Schiff base (Váró and Lanyi, 1991). It has been confirmed that the major conformational change occurs during M_1-to-M_2 transition (Sass et al., 1997). Furthermore, a subtle but essential conformational change occurs during the M_2-to-N transition, which is hydration dependent (Kamikubo et al., 1997). The displacement of the E-F loop may be as high as 5 Å (Thorgesirsson et al., 1997).

The structural change at helix F appears as a pair of positive and negative peaks. From this feature it seems that the cytoplasmic end of this helix moves away from the main body of the protein. Subramaniam et al. (1993) suggested that the movement of helix F opens a channel to transport a proton from the cytoplasmic surface into the protein. Ludlam et al. (1995) suggested that the Y185 to P186 region may function as a hinge for this movement. Consequently, there is a possibility that some water molecules enter the cytoplasmic channel and lower the pK_a of D96 (Kamikubo et al., 1997). On the other hand, there have been few investigations of the structural changes at the other helices.

Received for publication 13 July 1998 and in final form 20 October 1998.

Address reprint requests to Dr. Mikio Kataoka, Department of Materials Science, Nara Institute of Science and Technology, 8916-5, Takayama-machi, Ikoma, Nara 630-0101, Japan. Tel.: +81-743-72-6100; Fax: +81-743-72-6109; E-mail: kataoka@ms.aist-nara.ac.jp.

Dr. Kamikubo's present address is Institute of Materials Structure Science, High Energy Accelerator Research Organization, Tsukuba 350-0801, Japan.

0006-3495/99/02/1018/06 $2.00

Although all of the diffraction studies demonstrated a density change at helix G, the essence of this change remains unclear. Unlike the case of helix F, the change at helix G is characterized as a prominent positive peak without an accompanying unique and localized negative peak, which would be expected from a tilt. Instead, there is a series of small negative peaks (Subramaniam et al., 1993). The change at helix B is also characterized by a single distinct positive peak (Nakasako et al., 1991). To elucidate these structural changes in detail, experiments with higher resolution are required.

X-ray diffraction of heavy-atom-labeled BR is one of the promising methods for describing these structural changes in the required detail. If we can observe a change in a heavy-atom position in a specific intermediate, the essence of the structural change can be described in terms of amino acid residues. For this purpose, we introduced a single cysteine residue replacement substitution in BR, and the introduced cysteine was labeled with the organic mercury compound *p*-chloromercuribenzoate (PCMB). It has already been demonstrated that the position of a heavy atom can be determined within 1 Å (Krebs et al., 1993; Oka et al., 1997). We found that the mercury atoms were located at the positions expected from the high-resolution structure (Oka et al., 1997; Grigorieff et al., 1996). We have now extended the heavy-atom labeling method to the study of the structural change in the BR photocycle. We focused on the change in helix G, using the I222C BR mutant. The results show that in the M_N intermediate the mercury label at C222 moves 2 Å toward helix F.

MATERIALS AND METHODS

Sample preparation

The site-specific mutation I222C was introduced into the bop gene, and the changed gene was constructed by inserting it into a nonintegrating vector, with novobiocin resistance as the selective marker. *Halobacterium salinarium* was transformed as before (Ni et al., 1990; Needleman et al., 1991). The mutated protein was purified from *H. salinarium* as purple membrane (PM) sheets according to a standard method (Oesterhelt and Stoeckenius, 1974). PCMB labeling was described as before (Oka et al., 1997). PMs were suspended in 20 mM Na_2CO_3/$NaHCO_3$ buffer (pH 9.5) containing 10 mM NaCl.

X-ray diffraction experiment

The PM films for the x-ray diffraction were prepared on mylar sheets as discribed (Kamikubo et al., 1996; Oka et al., 1997) and equilibrated at 84% relative humidity. To transfer guanidine hydrochloride (Gdn-HCl) into the films, they were soaked for 10 min in a 100 mM Gdn-HCl solution (pH 9.5, containing 20 mM Na_2CO_3/$NaHCO_3$ and 10 mM NaCl), and thereafter the excess solution was removed (Dencher et al., 1989; Hauss et al., 1994). The films were equilibrated at 84% relative humidity for ~1 day. X-ray diffraction experiments were carried out with the MUSCLE Diffractometer (Amemiya et al., 1983) installed at BL15A in the Photon Factory, using synchrotron radiation as described previously (Nakasako et al., 1991). X-ray diffraction profiles were recorded at the same position of the same specimen, with and without continuous illumination with a 1-kW slide projector, using a cutoff filter Y-51 (transmission > 510 nm; Toshiba). The temparature of the sample was kept at 20°C. Exposure times were 180 s. Data are for reflections up to (7,1), which corresponds to 7-Å resolution.

Data refinement

X-ray data treatments and analysis are as described before (Oka et al., 1997). The electron distribution of the label comes mainly from the mercury atom, and for this reason we treated the electron density distribution of mercuribenzoate as a Gaussian. The structure factor of mercuribenzoate is

$$\mathbf{f}(hk) = A \exp(-BS^2)\exp[-2\pi i\,(hx + ky)].$$

A and B are the scale factor and the temperature factor, and h and k are Miller indices. Mercuribenzoate locates at (x, y). The structure factor of the labeled sample, $\mathbf{F}_H^{cal}(hk)$, is expressed as

$$\mathbf{F}_H^{cal}(hk) = \mathbf{F}_N(hk) + \mathbf{f}(hk) \quad (1)$$

where $\mathbf{F}_N$ is the observed structure factor of the nonlabeled sample. In the first step of the refinement, the following quantity is minimized:

$$\chi^2 = \sum_{hk} \frac{[|\mathbf{F}_H^{obs}(hk)|^2 - k|\mathbf{F}_H^{cal}(hk)|^2]}{\sigma_H^2 + \sigma_N^2}$$

where k and σ are the scale factor (in this case, nearly equal to 1) and the standard deviation of the observed intensity. The heavy-atom position is estimated by this procedure. In x-ray powder diffraction, the diffraction lines that have the same $h^2 + hk + k^2$ values appear at the same position. Therefore, the observed integral intensity of such a reflection line is a sum of overlapping reflections. Given the structure factor of the overlapping reflections as $\mathbf{F}_H(h_1k_1)$ and $\mathbf{F}_H(h_2k_2)$, the observed diffraction intensity can be written as

$$I(S) = |\mathbf{F}_H(h_1k_1)|^2 + |\mathbf{F}_H(h_2k_2)|^2 \quad (2)$$

Each structure factor of overlapping reflection was evaluated using the intensity ratios for reflections with the same $h^2 + hk + k^2$ for wild-type BR derived from cryoelectron microscopy data (Grigorieff et al., 1996). We recalculated the structure factors of the overlapping reflections for the labeled BR by using Eqs. 1 and 2 and the structure factor of mercury, $\mathbf{f}(hk)$, as the second part of refinement. The first and second parts of the refinement procedure were iterated alternately until good convergence was obtained. Data of 10 measurements of labeled I222C and eight measurements of nonlabeled I222C were averaged, and the errors were estimated. The lattice constant used was 62.45 Å (Grigorieff et al., 1996). The phases of the electron cryomicroscopy data (Henderson et al., 1990) were used for the difference electron density maps. The refinements of the labeled positions were performed independently for the M_N and BR states.

FTIR measurements

The samples for Fourier transform infrared (FTIR) measurements were prepared under the same conditions as for x-ray diffraction. A 6-μl sample of labeled or nonlabeled I222C BR suspended in 20 mM sodium carbonate buffer (pH 9.5) containing 10 mM NaCl was placed on a BaF_2 window (10-mm diameter) and dried under gentle stream of N_2 gas. To transfer Gdn-HCl into the films, they were soaked for 10 min in a 100 mM Gdn-HCl solution (pH 9.5, containing 20 mM Na_2CO_3/$NaHCO_3$ and 10 mM NaCl), and thereafter the excess solution was removed. The film was incubated under 84% relative humidity and sealed with silicone rubber spacer and another BaF_2 window. Spectral recordings were performed in a Horiba FT-210 Fourier transform infrared spectrophotometer equipped with an MCT detector. The temperature of the sample was kept at 20°C. The M_N intermediate was produced by irradiation of BR with >510-nm light for 30 s. Difference FTIR spectra were obtained with a 2-min recording after irradiation.

RESULTS

The difference density maps calculated from the intensity differences between M_N and BR are given in Fig. 1. The solid contour lines indicate regions of increased density, and the dotted lines the regions of decreased density in the M_N state. The positions of the helices and the arrangement of the BR monomers in the trimer are also indicated. The difference of the positive peak height near helix F between M_N and BR is ~3%. The map of nonlabeled I222C exhibits changes mainly at helices F and G with a minor change in helix B, which is the general property of N-type structure (Kamikubo et al., 1997). The positive peak near helix F is paired with a negative feature between helices F and G. In contrast, the positive peak of helix G is surrounded by several negative regions. These are the same changes as in the D96N mutant and the Gdn-HCl-treated wild-type BR at alkaline pH (Koch et al., 1991; Dencher et al., 1989). A change in density is also seen at helix B, but its amplitude is smaller. These features resemble the changes in the N intermediate (Kamikubo et al., 1996), consistent with the conclusion from FTIR results that M_N and N intermediates have similar structures (Sasaki et al., 1992). We had shown earlier that the structure of the M (M_2) intermediate is distinguishable from that of M_N or N, and the transition between the M-type structure and the N-type structure is hydration dependent (Kamikubo et al., 1997). In the present case, we used a relative humidity of 84% for the accumulation of the M_N intermediate, which seems rather low compared with the previous study (Kamikubo et al., 1997). However, the diffraction and FTIR spectra (Fig. 2) indicated the accumulation of the M_N intermediate. This would be partly because deliquescent Gdn-HCl brings sufficient water molecules to BR to accumulate the N-type conformation at a lower vapor pressure.

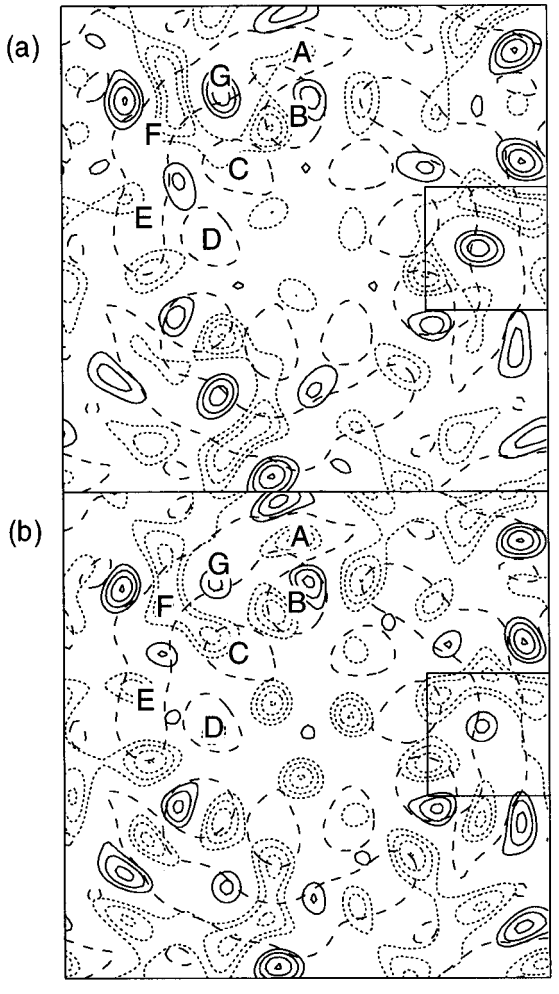

FIGURE 1 Difference density map between the M_N intermediate and the BR state. (*a*) Nonlabeled I222C BR. (*b*) PCMB-labeled I222C BR. The four solid contour lines indicate 70, 80, 90, 99% density change and the four dashed lines 1, 10, 20, 30%, where the maximum and minimum of the difference density are set as 100% and 0%. The outlines of the helices of BR and the trimer are also shown. The boxed region indicates the region enlarged in Fig. 4.

The difference map of labeled I222C differs somewhat from the map of the nonlabeled protein. The major difference is the lower amplitude of the change at helix G for the labeled protein. As discussed below, both Cys^{222} and the label are located at helix G, and the movement of the mercury label from the region of density increase into the neighboring region of negative density change compensates for increase due to the protein. It seems that this accounts for the difference, and otherwise the two density maps are very similar.

Fig. 2 shows the difference FTIR spectra between before and after illumination for the nonlabeled and the labeled I222C BR. The experimental conditions are the same as those for x-ray diffraction measurements, except for the continuous illumination for diffraction. The two curves show the same features. There is a pair of characteristic positive and negative amide I bands at 1650 and 1670 cm^{-1}. The COOH vibration of D85 is also observed at 1756 cm^{-1}. These features are diagnostic for the N-type protein conformation (Pfefferlé et al., 1991; Ludlam et al., 1995). The deprotonated state of the Schiff base is clear from the fact that no positive peak is observed at 1186 cm^{-1}. This FTIR evidence is consistent with the M_N intermediate state

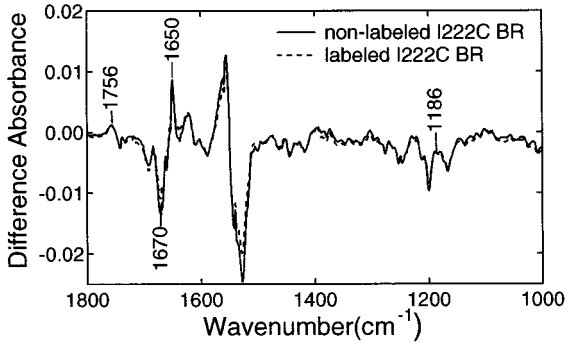

FIGURE 2 FTIR difference spectra between M_N intermediate state and BR state. The solid line indicates nonlabeled I222C BR, and the dashed line labeled I222C.

(Sasaki et al., 1992). It is confirmed by both difference Fourier map and difference FTIR spectra that the intermediate accumulated by illumination after Gdn-HCl treatment is the M_N intermediate.

The difference map between the labeled and nonlabeled I222C in the BR state clearly shows the density of the mercury atom (Fig. 3 *a*). We can see the single peak of the mercury at helix G in each monomer. It is broader than the peak observed for neutral pH (Oka et al., 1997), but the peak positions are same. The map of mercury density in the M_N state is shown in Fig. 3 *b*. It shows that the position of the mercury moves in the M_N-to-BR transition. This is consistent with the change at helix G in Fig. 1. The 3D difference map between N and BR shows the region near Ile^{222} as changes, mostly at helix G (Vonck, 1996). Because N has the same protein structure as M_N (Kamikubo et al., 1996), this result is in accord with the movement of mercury at Cys^{222}.

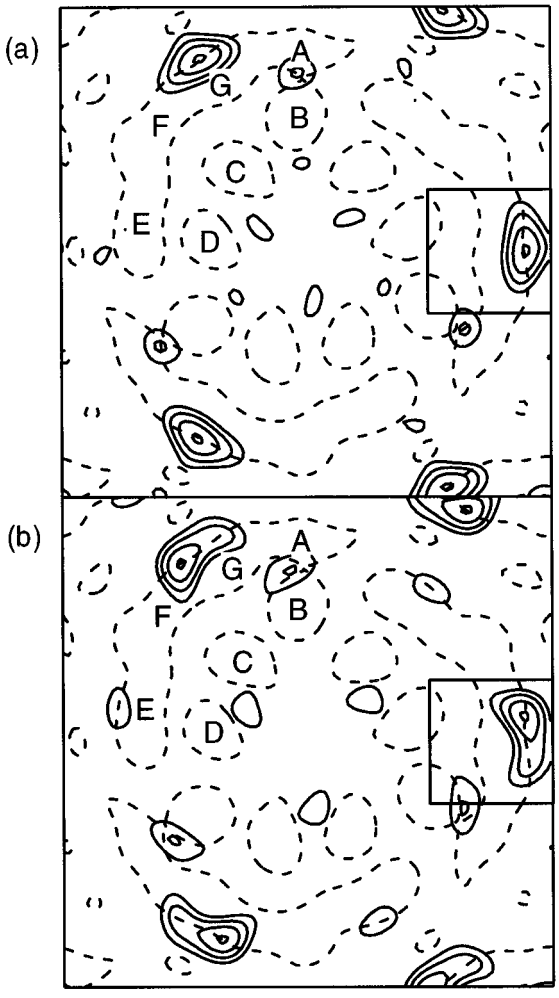

FIGURE 3 Difference density map between labeled and nonlabeled I222C BR. (*a*) BR state. (*b*) M_N state. The four solid contour lines indicate 70, 80, 90, 99% density change, where the maximum and minimum of the difference density are set at 100% and 0%. All noise peaks observed are shown in this figure. The boxed region indicates the region enlarged in Fig. 4.

After the positions of the mercury were roughly estimated from the initial difference map, the position refinements were performed with the method as described above (Oka et al., 1997). The coordinates of the refined positions are listed in Table 1. The coordinate system employed is the same as that of Grigorieff et al. (1996). The errors of these data are smaller than 1 Å. The mercury peak position of the BR state is the same as at neutral pH, within this error level (Oka et al., 1997). The mercury atom is located at the δ position of the cysteine residue. The position of the mercury differs by ~1.7 Å from the Ile^{222} δ atom in the wild-type BR structure (Grigorieff et al., 1996). This difference might arise from the labeling or the cysteine substitution.

The in-plane position of the mercury atom, and the 221st to the 223rd wild-type BR residues (Grigorieff et al., 1996) are shown in Fig. 4. Although in the new structure model (Luecke et al., 1998) some regions are different from the earlier structural model (Grigorieff et al., 1996), the structure of the region from the 221st to the 223rd residues is almost identical in these two structural models. We can see that the mercury atom is clearly moved in M_N relative to BR. The magnitude of the displacement of the mercury position in the BR-to-M_N transition is 2.1 ± 0.8 Å (Table 1). This value well exceeds the error level. The direction of the movement is toward the side of helix F that faces the center of the protein. The transition is from the positive region to the negative region in Fig. 1 *a*. This must be the reason why the positive peak is smaller in Fig. 1 *b*. The line connecting the center of helix G of the BR state and the center of the positive peak is parallel to the displacement vector of the mercury. The distance between the center of the positive peak and the main chain of helix G of the side of I222 to L223 is 2 Å, i.e., roughly equal to the mercury displacement, suggesting a shift in helix G during the BR-to-M_N transition.

DISCUSSION

Labeling and diffraction methods have been applied to investigate BR structure. Plöhn and Büldt (1989) showed that these methods can produce the labeled atom position with high accuracy, despite the low resolution of the data. In fact, deuterium labeling and neutron diffraction have been used to investigate structural changes in the BR photocycle. Hauss et al. (1994) labeled retinal with deuterium and detected its tilt after photoisomerization. The position of PCMB label in cysteine-substituted BRs has been studied at neutral pH in the unphotolyzed state (Krebs et al., 1993; Oka et al., 1997). These reports demonstrated that the mer-

TABLE 1 The refined coordinate of mercury atom positions in the M_N and BR states and its difference

	BR	M_N	M_N minus BR
X	27.78 ± 0.72	26.88 ± 0.60	−0.90 ± 0.94
Y	1.15 ± 0.60	3.02 ± 0.41	1.87 ± 0.73

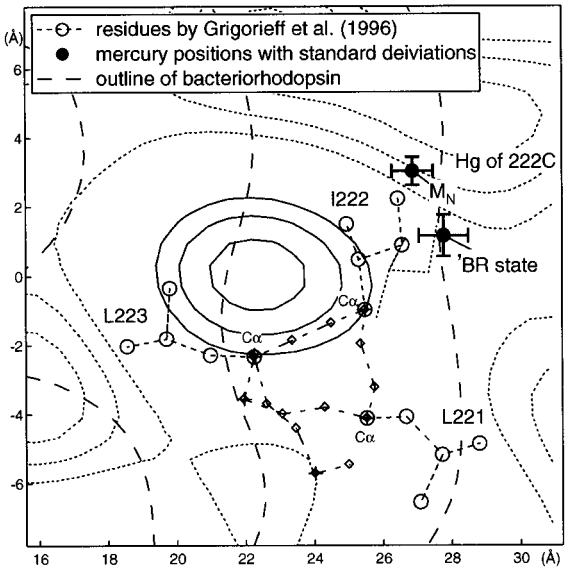

FIGURE 4 Mercury atom positions are shown in the M_N intermediate and the BR state. Error bars of position are also indicated. Wild-type BR residues (Grigorieff et al., 1996) from the 221st to the 223rd residues are shown. The nonlabeled I222C density change map (Fig. 1 *a*) is superimposed.

cury labeling method can provide precise information about the BR structure. We now used the same method with Gdn-HCl-treated labeled I222C BR and detected its position change during the photocycle. The error levels of the position of the label are almost the same as those at neutral pH (Oka et al., 1997). We show that the single mercury atom moves 2.1 ± 0.8 Å in the M_N photointermediate. This is the first report on detection of a movement of a specific amino acid residue in the BR photocycle by heavy atom labeling.

A structural change in the G helix had been observed in the M and the N intermediates before (Dencher et al., 1989; Koch et al., 1991; Nakasako et al., 1991; Subramaniam et al., 1993; Vonck, 1996; Kamikubo et al., 1996). Recently, the high-resolution BR structure has been reported by several groups using cryoelectron microscopy (Grigorieff et al., 1996; Kimura et al., 1997) and x-ray crystal structure analysis (Pebay-Peyroula et al., 1997; Luecke et al., 1998). According to these structures, helix G has a kink at around K216 to which retinal chromophore is bound. Vonck (1996) showed that the structural change in helix G occurs mainly in the cytoplasmic half, starting from G220. The most changed part in helix G is the region around I222. The extracellular side of helix G changes less than the cytoplasmic side. The present result indicates that the region around I222 of helix G moves toward helix F. Hauss et al. (1994) demonstrated that the β-ionone ring of retinal moves little, but the region near Schiff base moves 1.4 ± 0.9 Å toward the β-ionone ring in the M_N intermediate, which is the same direction as the mercury movement revealed in this study. This suggests that the region between K216 and I222 in helix G moves cooperatively with the region near the Schiff base of the retinal. Takei et al. (1994) found that the side chain of K216 undergoes a conformational change during the photocycle. The change in helix G thus may originate from the region of K216 and the retinal. The application of the mercury labeling to the other residues of helix G promises to reveal the properties of this change.

If the position change for the mercury represents the change at helix G in Fig. 1, this change is a tilt of the helix toward the inner side of F helix and the membrane normal. Thus G helix would move toward the positive region in the difference map (Fig. 4). If the helix tilts by as much as 2 Å, the change must appear as a pair of positive and negative peaks. But the positive peak at helix G is not accompanied by a single, localized feature of negative density in the difference map. Instead, we see the positive peak surrounded by a large area of nonconnected negative regions. It seems that the change in helix G is more complicated than a simple tilt. Subramaniam et al. (1993) had suggested that the cytoplasmic portion of helix G is more ordered in the intermediate state. Indeed, the 3-D difference map of N intermediate (Vonck, 1996), the vertical resolution of which is 10.5 Å, showed that the most prominent positive change at helix G is at its cytoplasmic side, from about the 220th residue to the helical end, including the I222 residue. On the *xy* coordinates, the positive region overlaps with I222 and F219. In the high-resolution structure of BR, helix G appears to bend near K216, which is linked to the retinal (Grigorieff et al., 1996; Kimura et al., 1997; Pebay-Peyroula et al., 1997; Luecke et al., 1998). This region of the helix may be mobile.

This work was partly supported by a grant from the Ministry of Education, Science, Sports and Culture of Japan to MK. TO and HK are grateful for the fellowships from the Japan Society for the Promotion of Science for Japanese Junior Scientists. The x-ray diffraction experiments were performed under the approval of the Photon Factory Program Advisory Committee (proposal nos. 94G077 and 96G066).

REFERENCES

Amemiya, Y., K. Wakabayashi, T. Hamanaka, T. Wakabayashi, T. Matsushita, and H. Hashizume. 1983. Design of a small-angle x-ray diffractometer using synchrotron radiation at the photon factory. *Nucl. Instrum. Methods.* 208:471–477.

Dencher, N. A., D. Dresselhaus, G. Zaccai, and G. Büldt. 1989. Structural changes in bacteriorhodopsin during proton translocation revealed by neutron diffraction. *Proc. Natl. Acad. Sci. USA.* 86:7876–7879.

Grigorieff, N., T. A. Ceska, K. H. Downing, J. M. Baldwin, and R. Henderson. 1996. Electron-crystallographic refinement of the structure of bacteriorhodopsin. *J. Mol. Biol.* 259:393–421.

Hauss, T., G. Büldt, M. P. Heyn, and N. A. Dencher. 1994. Light-induced isomerization causes chromophore tilts in the M intermediate of bacteriorhodopsin: a neutron diffraction study. *Proc. Natl. Acad. Sci. USA.* 91:11854–11858.

Henderson, R., J. Baldwin, T. A. Ceska, F. Zemlin, E. Beckmann, and K. H. Downing. 1990. Model for the structure of bacteriorhodopsin based on high-resolution electron cryo-microscopy. *J. Mol. Biol.* 213: 899–929.

Kamikubo, H., M. Kataoka, G. Váró, T. Oka, F. Tokunaga, R. Needleman, and J. K. Lanyi. 1996. Structure of the N intermediate of bacteriorhodopsin revealed by x-ray diffraction. *Proc. Natl. Acad. Sci. USA.* 93: 1386–1390.

Kamikubo, H., T. Oka, Y. Imamoto, F. Tokunaga, J. K. Lanyi, and M. Kataoka. 1997. The last phase of the reprotonation switch in bacteriorhodopsin: the transition between the M-type and the N-type protein conformation depends on hydration. *Biochemistry.* 36: 12282–12287.

Kataoka, M., H. Kamikubo, F. Tokunaga, L. S. Brown, Y. Yamazaki, A. Maeda, M. Sheves, R. Needleman, and J. K. Lanyi. 1994. Energy coupling in an ion pump. The reprotonation switch of bacteriorhodopsin. *J. Mol. Biol.* 243:621–638.

Kimura, Y., D. G. Vassylyev, A. Miyazawa, A. Kidera, M. Matsushima, K. Mitsuoka, K. Murata, T. Hirai, and Y. Fujiyoshi. 1997. Surface of bacteriorhodopsin revealed by high-resolution electron crystallography. *Nature.* 389:206–211.

Koch, M. H., N. A. Dencher, D. Oesterhelt, H.-J. Plöhn, G. Rapp, and G. Büldt. 1991. Time-resolved x-ray diffraction study of structural changes associated with the photocycle of bacteriorhodopsin. *EMBO J.* 10: 521–526.

Krebs, M. P., W. Behrens, R. Mollaaghababa, H. G. Khorana, and M. P. Heyn. 1993. X-ray diffraction of a cysteine-containing bacteriorhodopsin mutant and its mercury derivative. Localization of an amino acid residue in the loop of an integral membrane protein. *Biochemistry.* 32:12830–12834.

Lanyi, J. K. 1995. Bacteriorhodopsin as a model for proton pumps. *Nature.* 375:461–463.

Lanyi, J. K. 1997. Mechanism of ion transport across membranes. Bacteriorhodopsin as a prototype for proton pumps. *J. Biol. Chem.* 272: 31209–31212.

Ludlam, C. F. C., S. Sonar, C.-P. Lee, M. Coleman, J. Herzfeld, U. L. Rajbhandary, and K. J. Rothschild. 1995. Site-directed isotope labeling and ATR-FTIR difference spectroscopy of bacteriorhodopsin: the peptide carbonyl group of Tyr 185 is structurally active during the bR→N transition. *Biochemistry.* 34:2–6.

Luecke, H., H. T. Richter, and J. K. Lanyi. 1998. Proton transfer pathway in bacteriorhodopsin at 2.3 Angstrom resolution. *Science.* 280:1934–37.

Nakasako, M., M. Kataoka, Y. Amemiya, and F. Tokunaga. 1991. Crystallographic characterization by x-ray diffraction of the M-intermediate from the photo-cycle of bacteriorhodopsin at room temperature. *FEBS Lett.* 292:73–75.

Needleman, R., M. Chang, B. Ni, G. Váró, J. Fornes, S. H. White, and J. K. Lanyi. 1991. Properties of Asp^{212}→Asn bacteriorhodopsin suggest that Asp^{212} and Asp^{85} both participate in a counterion and proton acceptor complex near the Schiff base. *J. Biol. Chem.* 266:11478–11484.

Ni, B., M. Chang, A. Duschl, J. K. Lanyi, and R. Needleman. 1990. An efficient system for the synthesis of bacteriorhodopsin in *Halobacterium halobium*. *Gene.* 90:169–172.

Oesterhelt, D., and W. Stoeckenius. 1974. Isolation of cell membrane of *Halobcterium halobium* and its fractionation into red and purple membrane. *Methods Enzymol.* 31:667–678.

Oka, T., H. Kamikubo, F. Tokunaga, J. K. Lanyi, R. Needleman, and M. Kataoka. 1997. X-ray diffraction studies of bacteriorhodopsin. Determines of the positions of mercury label at several engineered cysteine residues. *Photochem. Photobiol.* 66:768–773.

Pebay-Peyroula, E., G. Rummel, J. P. Rosenbusch, E. M. Landau. 1997. X-ray structure of bacteriorhodopsin at 2.5 angstroms from microcrystals grown in lipidic cubic phases. *Science.* 277:1676–1681.

Pfefferlé, J. M., A. Maeda, J. Sasaki, and T. Yoshizawa. 1991. Fourier transform infrared study of the N intermediate of bacteriorhodopsin. *Biochemistry.* 30:6548–6556.

Plöhn, H.-J., and G. Büldt. 1989. The determination of label positions in membrane proteins by neutron and anomalous x-ray diffraction of powder samples. *J. Appl. Crystallogr.* 19:255–261.

Sasaki, J., Y. Shichida, J. K. Lanyi, and A. Maeda. 1992. Protein changes associated with reprotonation of the Schiff base in the photocycle of Asp^{96} → Asn bacteriorhodopsin. *J. Biol. Chem.* 267:20782–20786.

Sass, H. J., I. W. Schachowa, G. Rapp, M. H. J. Koch, D. Oesterhelt, N. A. Dencher, and G. Büldt. 1997. The tertiary structural changes in bacteriorhodopsin occur between M states: x-ray diffraction and Fourier transform infrared spectroscopy. *EMBO J.* 16:1484–1491.

Subramaniam, S., M. Gerstein, D. Oesterhelt, and R. Henderson. 1993. Electron diffraction analysis of structural change in the photocycle of bacteriorhodopsin. *EMBO J.* 12:1–8.

Takei, H., Y. Gat, Z. Rothman, A. Lewis, and M. Sheves. 1994. Active site lysine backbone undergoes conformational changes in the bacteriorhodopsin photocycle. *J. Biol. Chem.* 269:7387–7389.

Thorgesirsson, T. E., W. Xiao, L. S. Brown, R. Needleman, J. K. Lanyi, and Y.-K. Shin. 1997. Transient channel-oepning in bacteriorhodopsin: an EPR study. *J. Mol. Biol*. 273:951–957.

Váró, G., and J. K. Lanyi. 1991. Thermodynamics and energy coupling in the bacteriorhodopsin photocycle. *Biochemistry.* 30:5008–5015.

Vonck, J. 1996. A three-dimensional difference map of the N intermediate in the bacteriorhodopsin photocycle: part of the F helix tilts in the M to N transition. *Biochemistry.* 35:5870–5878.